TÜBİTAK

Original Article

Turk J Med Sci
2012; 42 (5): 787-795
© TÜBİTAK
E-mail: medsci@tubitak.gov.tr
doi:10.3906/sag-1106-37

Chest radiography and computed tomography findings of cases with pandemic influenza A (H1N1/09) infection

Pınar Nercis KOŞAR[1], Zeliha KOÇAK TUFAN[2], Elif ERGÜN[1], Hasan YİĞİT[1], Uğur KOŞAR[1], Ali Pekcan DEMİRÖZ[2]

Aim: To review the radiological findings of the chests of swine flu patients whose infections were confirmed clinically and/or by laboratory tests.

Materials and methods: This study was conducted in the radiology and infectious diseases departments of a tertiary care hospital, Ankara Training and Research Hospital, Ankara, Turkey. The X-ray and thorax computed tomography (CT) findings of swine flu patients were evaluated.

Results: Included were 53 cases of swine flu. Thirty-eight of the patients (72%) underwent an initial chest X-ray and 17 (32%) underwent thorax CT examinations. The mean age of the patients was 41 years; 23 (43%) patients were male and 30 (57%) were female. In the chest X-rays, the most common pathology was patchy consolidations with a prevalence of 27%. Bilateral symmetrical involvement was observed in 42% of the cases. In the thorax CT, patchy consolidations (47%) and ground glass opacification (24%) were the most commonly observed patterns. Bilateral symmetrical involvement was observed in 41% of the cases. Pleural effusion was seen in 29% of the cases and mediastinal lymphadenopathy was observed in 41% of the cases.

Conclusion: The most commonly observed radiological pattern of influenza A (H1N1) pulmonary infection is bilateral, symmetrical, patchy consolidations and/or ground glass opacities, predominantly located in middle-inferior zones with central peribronchovascular distribution. Associated mediastinal lymph nodes, pleural effusion, and tree-in-bud patterns should raise the suspicion of superimposed infection.

Key words: Influenza A (H1N1), epidemics, radiology findings

Introduction

Novel influenza A virus, pandemic (H1N1) 2009, has been identified as the cause of the influenza outbreak in 2009 throughout the world (1). Since the beginning of the 20th century, there have been 4 or 5 influenza pandemics. The Spanish flu pandemic of 1918 was also caused by the human influenza A (H1N1) virus and resulted in 40-50 million deaths (2). In 2009, more than 208 countries reported laboratory-confirmed cases of pandemic influenza H1N1 and at least 13,554 deaths (3). The most common symptom of this pandemic was fever, followed by cough, nausea, headache, vomiting, and diarrhea (4). Some patients had severe pneumonia and even respiratory failure, which required mechanical ventilation (5).

In Turkey, according to Ministry of Health reports, between 12 November and 31 December 2009, 13,111 patients were hospitalized due to H1N1 infection, of which 2721 patients were admitted to intensive care units and 1161 patients required

Received: 14.06.2011 – Accepted: 17.11.2011

[1] Department of Radiology, Ankara Training and Research Hospital, Ankara - TURKEY
[2] Department of Infectious Diseases and Clinical Microbiology, Ankara Training and Research Hospital, Ankara - TURKEY
Correspondence: *Zeliha KOÇAK TUFAN, Department of Radiology, Ankara Training and Research Hospital, Ulucanlar 06340, Ankara - TURKEY*
E-mail: drztufan@yahoo.com

mechanical ventilation (6). Between 19 October and 6 December 2009, 320 deaths were confirmed to be due to H1N1 (7).

Being familiar with the radiological findings of the chest in patients with H1N1 infection is important for early diagnosis and effective treatment planning in these patients. Although chest radiographic findings of H1N1 are described thoroughly in the literature, there are few reports on thorax computed tomography (CT) findings in patients with presumed or confirmed H1N1 infection. The purpose of this study was to review the radiological findings of the chest in hospitalized H1N1 patients whose infections were confirmed clinically and/or by laboratory tests.

Materials and methods

Among the patients who were admitted to our hospital with swine flu symptoms between 29 October 2009 and 6 January 2010, 53 patients were hospitalized due to H1N1 infection. These cases, which were confirmed clinically and/or by laboratory tests, were the subjects of this study. Ethics approval for the study was given by the hospital. Outpatients and patients in the pediatric age group were excluded.

Laboratory confirmation of H1N1 was done using real-time reverse transcriptase polymerase chain reaction (RT-PCR). A combined nasopharyngeal and oropharyngeal swab was used. For patients that were intubated, an endotracheal aspirate was also collected. Clinical diagnosis of influenza was done according to US Centers for Disease Control and Prevention guidelines. The patients either had laboratory confirmation of H1N1 infection or were presumed to have H1N1 infection (even with negative laboratory tests) based on the clinical findings and the fact that no other viruses were circulating in the community at any frequency at that time.

Of the 53 patients, 38 (72%) underwent an initial chest X-ray in our institution, whereas 8 were followed clinically without a chest X-ray due to pregnancy (either they were in the early period or declined to have an X-ray) and 7 were referred from other hospitals without an initial chest X-ray. Of the 38 patients with an initial chest X-ray, 17 (32% of the total) underwent thorax CT examinations. The average time interval between the initial chest X-ray and the thorax CT was 4 days (range: 0-9 days). Those who were clinically stable and/or pregnant did not undergo a CT examination.

Fourteen of the 17 CT examinations were performed using a 64-slice CT scanner (Toshiba Aquilion 64) with 120 kV, 150 mA, 5-mm section thickness, and 5-mm increment, whereas 3 were performed using a single-slice CT scanner (Hitachi Pronto SE) with 120 kV, 175 mA, 10-mm section thickness, and 10-mm increment. In 14 patients (82%), 100 mL of intravenous (IV) contrast agent (Omnipaque 300, GE Healthcare; Ultravist 300, Schering) was injected before the CT scan.

Two radiologists with 15-20 years of experience in thorax radiology reviewed the chest X-rays and thorax CT examination results. The radiological examinations were grouped as normal and abnormal. Abnormal findings were characterized as consolidation (opacification obscuring the underlying parenchymal architecture), ground glass opacification (GGO; underlying parenchymal architecture remained visible), and linear and nodular opacities and mixed patterns (combined alveolar densities and linear opacities). These were classified as unilateral or bilateral, and the bilateral cases were further classified as symmetrical or asymmetrical. Localization of the lesions in the chest X-rays was defined by dividing the parenchyma into 3 zones as upper, middle, and lower. In the thorax CT examinations, the region of parenchyma from the apex to the carina was defined as the upper zone, the region distal to the inferior pulmonary vein was defined as the lower zone, and the region in between was defined as the middle zone. The distribution of the lesions was classified as central, peripheral, or diffuse. The presence of pleural effusion and enlarged lymph nodes were explored and noted. The 14 patients to whom IV contrast agent was administered were also evaluated for pulmonary embolism. In all of the patients, secondary bacterial pulmonary infections, congestive heart failure, volume overload, or an underlying pulmonary disease, which may mimic the chest radiological findings of H1N1 infection, were evaluated clinically and/or by laboratory tests.

Results

The mean age of the patients was 41 years (16-88 years), 23 (43%) were male, and 30 (57%) were female. The RT-PCR test was positive in 30 (57%) of the cases, while in 23 (43%) it was negative, and H1N1 infection was diagnosed based on the clinical findings.

Chest X-ray findings

X-ray results are shown in Figures 1-3. Of the 38 patients who had initial chest X-rays, 5 (13%) showed normal findings, while 33 (87%) showed positive radiographic findings. Of these 33 patients, 15 (46%) had consolidation (9/15 patchy, 6/15 diffuse consolidation), and 7 (21%) of the patients had GGO. When both consolidation and GGO were detected in the same case, the case was classified according to the dominant finding. Linear opacities were observed in 5 (15%) cases, of which 2 had minimal opacities. Mixed pattern was observed in 6 (18%) cases (in 5 of these, the linear opacities were predominant, while in 1, GGO was predominant). The most common radiological finding was patchy consolidations with a prevalence of 27% (9/33) (Figures 1a, 2a, and 3a). Unilateral involvement was present in 10 (30%) cases and bilateral involvement was present in 23 (70%) cases. Among the 23 cases with bilateral lesions, involvement was symmetrical in 14 (61%). Bilateral symmetrical involvement in chest X-ray was observed in 42% of the cases (Figure 2a). The distribution of the lesions was central in 22 (67%) cases, while peripheral and diffuse distribution was observed in 5 (15%) and 6 (18%) cases, respectively. When zonal anatomy was considered, the lesions were localized in the upper zone in 1 (3%) case, in the middle zone in 4 (12%) cases, and in middle-inferior zone in 19 (58%) cases. Pleural effusion was seen in 6 (18%)

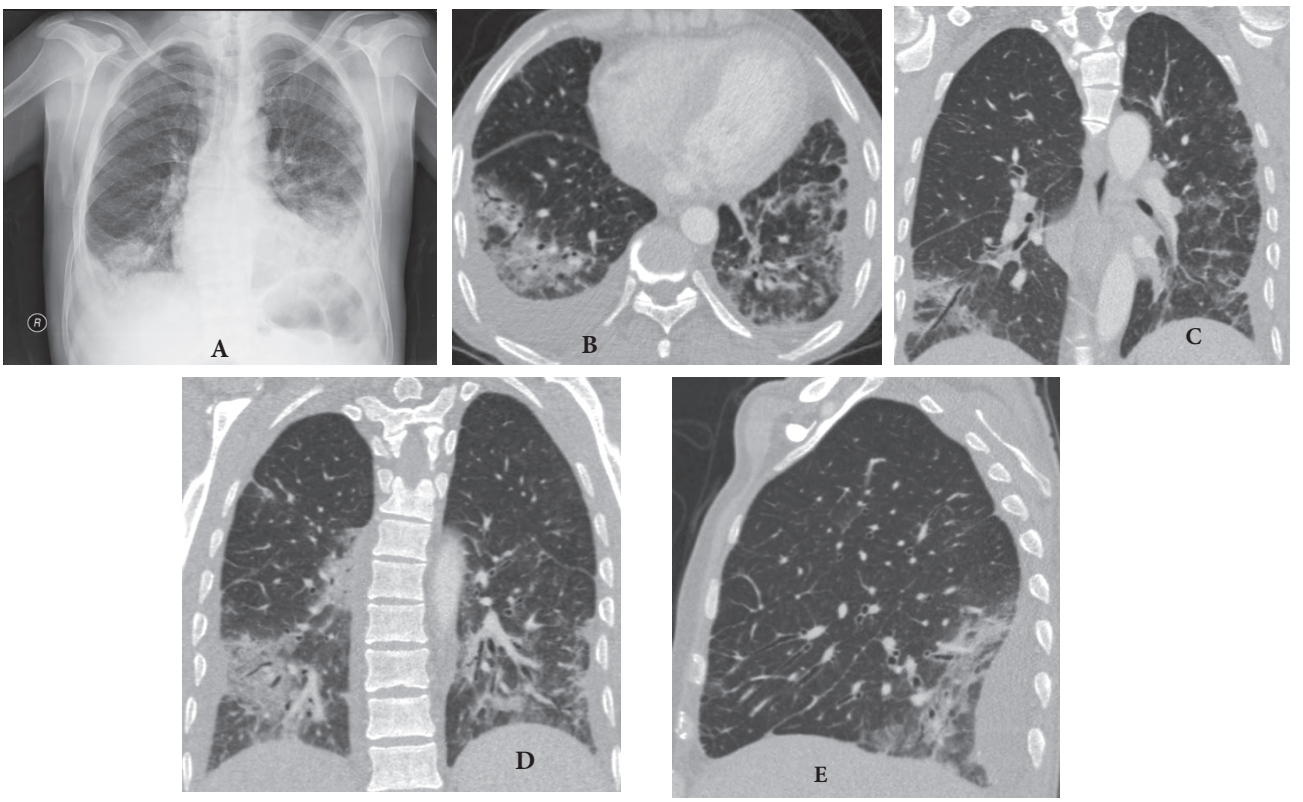

Figure 1. An 88-year-old male patient diagnosed with H1N1 pneumonia with superimposed infection and associated heart failure and volume overload. Initial chest X-ray (A) shows ill-defined infiltrates in both lower zones and left-middle zone; bilateral pleural effusion is also seen. Axial (B), coronal (C and D), and sagittal (E) chest CT images show bilateral asymmetric involvement of predominantly the inferior zones with patchy, peribronchial, ill-defined consolidations and air bronchograms. Bronchial wall thickening is associated. Accompanying bilateral thickening of the major fissures, pleural effusion, and interlobular septal thickening indicate volume overload.

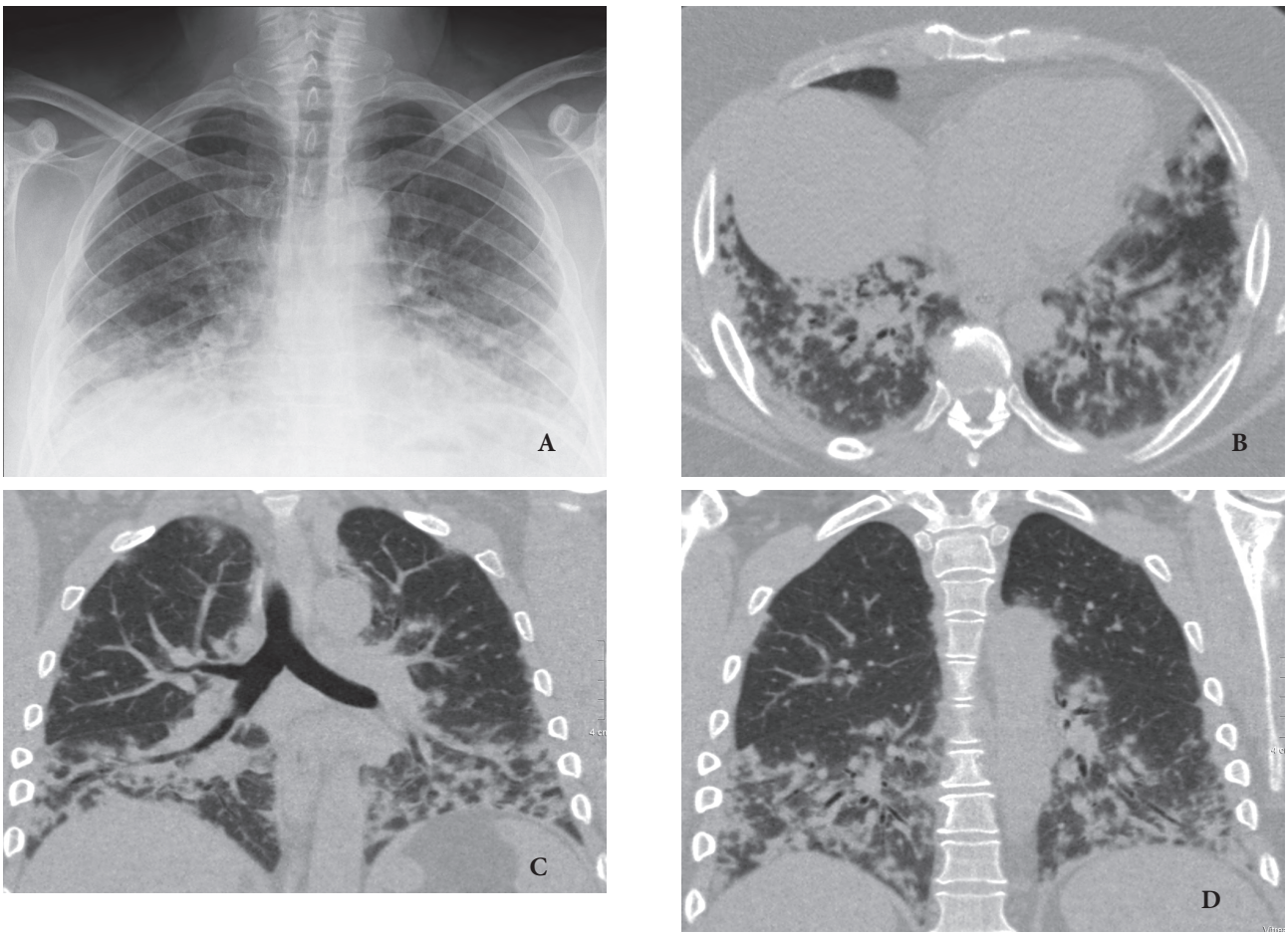

Figure 2. A 36-year-old male patient diagnosed with H1N1 pneumonia and secondary infection. Posteroanterior chest X-ray (A) shows bilateral, symmetrical, ill-defined, multifocal opacities in middle-inferior zones. Axial (B) and coronal (C and D) CT images show bilateral, symmetrical, peribronchial, and perilobular infiltration localized in middle-inferior zones with peripheral and central distribution. Associated bronchial wall thickening and tree in bud pattern are also seen.

cases. Lymph node enlargement was not detected in any of the cases. The findings of the chest X-rays are summarized in Table 1.

Thorax CT findings

Of the 17 patients that underwent thorax CT examinations, 9 (53%) had consolidation (8/9 patchy, 1/9 diffuse). In 2 of these cases, GGO was present apart from patchy consolidations (Figures 3b, 3c, and 4). In 4 (24%) cases only GGO was observed (Figure 5). Linear opacities were observed in 1 (6%) case, while a mixed pattern was present in 3 (18%) cases. Among the cases with a mixed pattern, linear opacities were predominant in 2, whereas GGO was the predominant pattern in 1, and associated centrilobular densities (tree-in-bud pattern) were seen in 1 case (Figures 2b and 2d). In 4 (24%) cases, left unilateral involvement was present. Bilateral involvement was present in 13 (76%) cases, of which 7 had symmetrical involvement (Figure 4) and 6 had asymmetrical involvement (Figures 1b and 1e). The lesions were distributed centrally in 9 (53%) cases, whereas peripheral and diffuse distribution were observed in 3 (18%) and 5 (29%) cases, respectively. In 1 (6%) case, lesions were located in the upper zone; in 4 (24%) cases, they were located in the middle zone; and in 5 (29%) cases, they were located in the middle-inferior zone. In 2 cases, extensive involvement in all 3 zones was observed. Pleural effusion was seen in 5 (29%) cases and mediastinal lymph node enlargement was observed in 7 (41%)

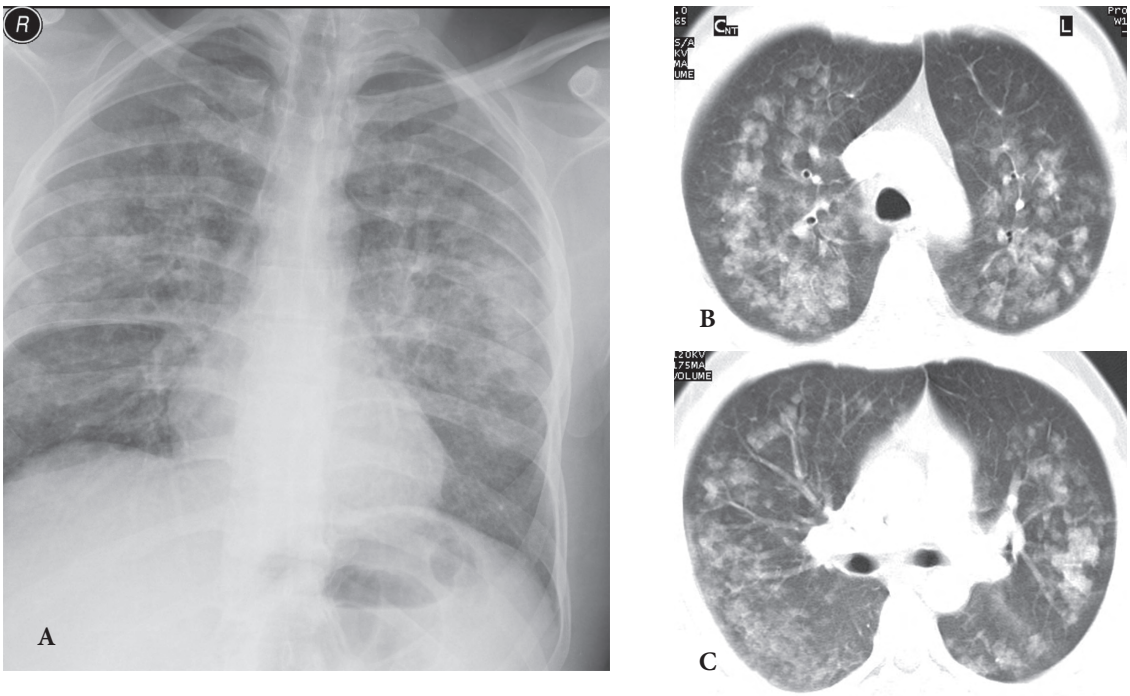

Figure 3. A 35-year-old male patient. Posteroanterior chest X-ray (A) reveals that the upper and middle zones of both lungs show predominantly patchy consolidations with interposed nodular pattern. Axial chest CT images (B and C) show, bilateral, symmetrical, rounded ground glass opacities and consolidations in peribronchovascular distribution.

Table 1. Radiographic findings of the 38 cases with initial chest X-ray.

	Number of cases	Percentage of cases (%)
Abnormal findings in chest X-ray	33/38	87
Unilateral involvement	10/33	30
Right	2/10	20
Left	8/10	80
Bilateral involvement	23/33	70
Bilateral symmetrical	14/23	61
Bilateral asymmetrical	9/23	39
Localization		
Central	22/33	67
Peripheral	5/33	15
Central + peripheral	6/33	18
Zone		
Upper	1/33	3
Middle	4/33	12
Inferior	8/33	24
Middle-inferior	19/33	58
Diffuse	1/33	3
Pattern		
Consolidation	15/33	46
Diffuse	6/15	40
Patchy	9/15	60
Ground glass opacification	7/33	21
Linear opacities	5/33	15
Mixed pattern	6/33	18
Pleural effusion	6/33	18

cases. In 4 cases, both of these findings were present. Thorax CT findings are presented in Table 2 and the clinical characteristics and radiological findings of each case with thorax CT are presented in Table 3.

Pulmonary embolism was not observed in any of the cases. Four cases had additional findings such as paravertebral mass, thin-walled air cysts, diaphragm hernia, and multiple cysts or hydatid cyst in the liver.

In 2 of the cases, mechanical ventilation was needed. One patient with a poor clinical status due to a cerebrovascular event died. All of the other patients recovered with treatment.

Discussion

Pandemic and seasonal influenza are usually self-limited diseases. However, in some cases, upper respiratory tract infections rapidly progress into fatal pulmonary disease. In these patients, hospitalization and mechanical ventilation is required (8). To predict in which of the patients the disease will result in respiratory distress is not possible. As a distinction from previous pandemics, the current pandemic H1N1 influenza has been more fatal in young healthy adults (5,9). Especially in patients with false negative RT-PCR test results, the consequent delay in the

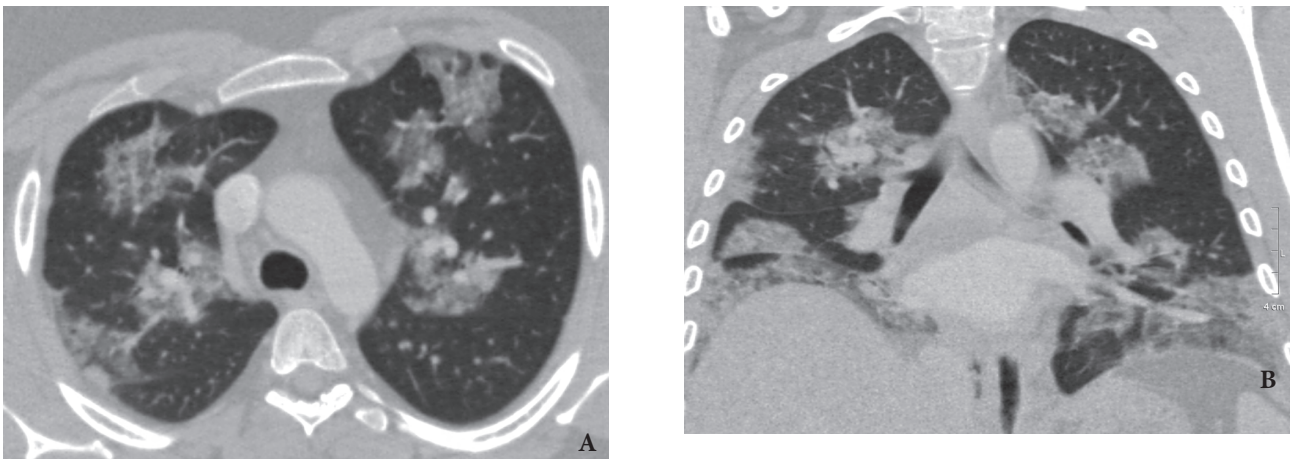

Figure 4. A 29-year-old male patient diagnosed with H1N1 pneumonia without secondary infection; bilateral, symmetrical, patchy ground glass opacities and consolidations in subpleural and peribronchovascular distribution are shown in axial (A) and coronal (B) chest CT images.

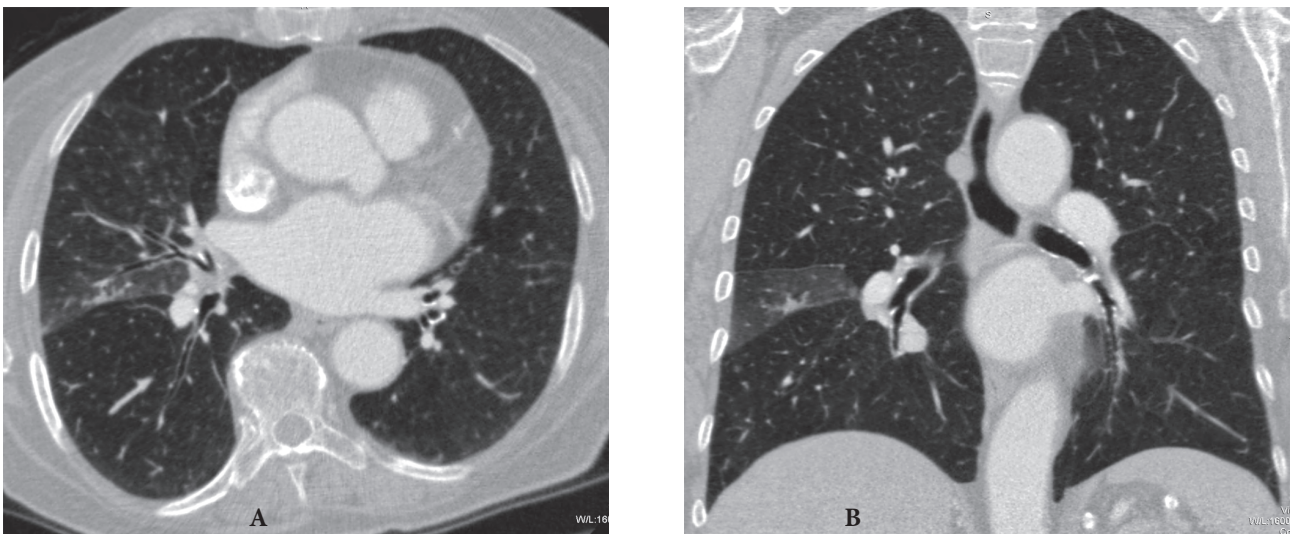

Figure 5. An 87-year-old female patient. Axial (A) and coronal (B) chest CT images depict GGO bordered by the major fissure, in the right middle lobe with associated bronchial wall thickening.

diagnosis and initiation of the appropriate antiviral therapy increases the mortality rate (10).

Nucleic acid amplification tests, including RT-PCR, are the most sensitive and specific tests used to confirm the diagnosis of H1N1 infection. However, false negative tests can occur, and clinical decisions and local surveillance data play a crucial role in the differential diagnosis of patients with influenza-like illness and a negative H1N1 test. Late admission to the hospital, already being on antiviral (oseltamivir) therapy, and the absence of sputum or bronchoalveolar lavage specimens are thought to be the main reason for false negative test results in our study population. Although we were able to get endotracheal aspirate samples from our intubated patients, we were not able to get lower respiratory tract samples from patients who were not intubated. In addition, we were able to get sputum samples for a limited number of our patients, all of whom already had positive RT-PCR results from the oropharyngeal and nasopharyngeal swabs.

Tracheitis, bronchiolitis, and diffuse alveolar damage have been reported in most cases of H1N1 infection. In the autopsy series of Gill et al. (11), which consisted of 34 H1N1 cases, viral pneumonia with focal to extensive diffuse alveolar damage (DAD) was observed in 25 of the cases. They also reported that there were associated marked hyaline membrane formations, pulmonary edema, and pulmonary hemorrhages, and in 55% of the cases superimposed bacterial pneumonia was present. Superimposed bacterial pneumonia makes the condition more complicated and requires changes in the treatment regime. Radiological findings may help to identify the patients who need hospitalization and may guide treatment. Specifically, thorax CT, which characterizes the lesions and shows their distribution in detail, has an important role in determining the

Table 2. Summary of radiological findings of 17 cases with thorax CT.

	Number of cases	Percentage of cases (%)
Unilateral involvement	4/17	24
Right	-	-
Left	4/4	100
Bilateral involvement	13/17	76
Bilateral symmetrical	7/13	54
Bilateral asymmetrical	6/13	46
Localization		
Central	9/17	53
Peripheral	3/17	18
Central + peripheral	5/17	29
Zone		
Upper	1/17	6
Middle	4/17	24
Inferior	5/17	29
Middle-inferior	5/17	29
Diffuse	2/17	12
Pattern		
Consolidation	9/17	53
Diffuse	1/9	11
Patchy	8/9	89
Ground glass opacification	4/17	24
Linear opacities	1/17	6
Mixed pattern	3/17	18
Pleural effusion	5/17	29
Mediastinal lymph nodes	7/17	41

Table 3. Clinical characteristics and radiological findings of cases with thorax CT.

No.	Age	Sex	Comorbidity	Secondary infection	Heart failure	Volume overload	Consolidation	GGO	Linear opacities	Pleural effusion	Lymph nodes
1	50	M	**History of tuberculous meningitis,COPD**	+	–	–	–	+	–	–	+
2	59	F	**COPD**	–	–	–	–	+	–	–	–
3	87	F	**COPD**	+	+	–	–	+	–	–	+
4	88	M	**COPD**	+	+	+	–	+	–	+	+
5	29	M	**Hypopituitarism, under steroid treatment**	–	–	–	+	–	–	–	–
6	44	F	–	+	–	–	–	+	+	–	+
7	36	F	–	+	–	+	+	–	–	+	+
8	83	M	–	+	+	–	–	+	+	+	+
9	46	M	**COPD, obesity**	+	+	+	+	–	–	–	–
10	47	M	–	+	–	–	+	+	–	+	+
11	50	F	–	–	–	–	+	–	–	–	–
12	32	M	–	–	–	–	+	–	–	–	–
13	35	M	–	–	–	–	+	+	–	–	–
14	39	M	–	+	–	–	+	–	+	+	–
15	31	M	–	–	–	–	+	–	–	–	–
16	64	F	**COPD**	+	+	+	–	–	+	–	–
17	38	M	**HIV+**	+	–	–	–	+	+	–	–

COPD: chronic obstructive pulmonary disease, **HIV**: human immunodeficiency virus, **GGO**: ground glass opacification

prognosis and planning the treatment and follow-up of the patients. In addition, radiological findings may prevent a delay in the diagnosis and initiation of therapy in patients with negative PCR results (10).

The most commonly defined radiological findings in H1N1 viral pneumonia are focal, multifocal, diffuse GGO, and/or consolidations (5,7-9). The predominant locations of these lesions are basal lobes with a central distribution (9). In accordance with the literature, the most common radiological findings in our study population were multifocal patchy consolidations and ground glass opacities. In addition, bilateral and symmetrical involvement was noticed in many cases (42% in chest X-rays, 41% in thorax CT). The lesions were predominantly located in middle-inferior zones (58% of chest X-rays) and had central distribution (67% in chest X-rays, 53% in CT). Linear opacities that extended from the pleural surface to the pulmonary hilar were also observed. Lesions with peripheral distribution were typically pleural-based patchy consolidations or ground glass opacities. This appearance has been observed to bear a resemblance to the organizing pneumonia (12). Resemblance between the radiological findings of H1N1 infection and severe acute respiratory syndrome (SARS) has been reported in the medical literature. The predominant radiological findings in both diseases are patchy consolidations and/or ground glass opacities. On the other hand, the centrilobular nodules, septal thickening and mediastinal and hilar lymph nodes that were reported in viral pneumonia cases were not reported in neither of these diseases (13). Lesion distribution in SARS was reported to be mostly peripheral, whereas in our series, peripheral distribution was observed in chest X-rays and CT only in 15% and 18% of the cases, respectively, and central distribution was predominant. Moreover, findings like reticular densities, traction bronchiectasis, and superimposed complications such as pneumomediastinum and pneumothorax, which are all observed in SARS, are not reported

in H1N1 infections (13). Although branching centrilobular opacities (referred to as tree-in-bud pattern) that can be observed in bacterial, viral, and mycoplasma pneumonia were not defined among the radiological features of H1N1 pneumonia, we observed this pattern in one of our cases. Moreover, in contrast to the cases reported in the literature, we detected mediastinal lymph nodes in 7 (41%) cases.

Pleural effusion was seen in chest X-rays and CT in 18% (n = 6) and 29% (n = 5) of our cases, respectively. Pleural effusion and interlobular septal thickening was reported to be due to fluid overload (8). However, in our study population, of the 4 cases with fluid overload and 5 cases with congestive heart failure, only 2 had pleural effusion, and, with the exception of 1 case, findings that indicated venous congestion were not present in any of the cases. Our cases with mediastinal lymph nodes, pleural effusion, and tree-in-bud pattern had superimposed bacterial infections; hence, in the presence these findings, the possibility of superimposed bacterial infection should not be overlooked.

In the series of Agarwal et al. (9), which consisted of 14 cases of H1N1 infection, 5 included pulmonary embolism. In our series, of the 14 patients that underwent thorax CT examination with intravenous contrast material administration, none had pulmonary embolism.

A limitation of this study was that we could not investigate the chest radiological features in the early phases of the disease or in the uncomplicated cases, because only hospitalized patients were included in the study. Another limitation was that the time interval between the beginning of the symptoms and admission to the hospital was not known; hence, the phase of the illness that carries the radiological findings defined in this study was not clear. Moreover, performing radiological evaluations after the clinical status had worsened resulted in superimposition of the radiological findings of H1N1 infection and the superimposed infection in most cases.

The clinical spectrum of H1N1 infection ranges from mild to fatal forms. Chest radiological findings and especially thorax CT made detailed identification of the alveolar damage possible. The most commonly observed radiological pattern of H1N1 pulmonary infection was patchy consolidations and/or GGO, predominantly located in middle-inferior zones with central peribronchovascular distribution. Involvement was usually bilateral and symmetrical. Associated mediastinal lymph nodes, pleural effusion, and tree-in-bud patterns should raise the suspicion of superimposed infection.

References

1. Centers for Disease Control and Prevention. Update: novel influenza A (H1N1) virus infections - worldwide. MMWR Morb Mortal Wkly Rep 2009; 58: 453-8.
2. Petrosillo N, Di Bella S, Drapeau CM, Grilli E. The novel influenza A (H1N1) virus pandemic: an update. Ann Thorac Med 2009; 4: 163-72.
3. World Health Organization. Pandemic (H1N1) 2009 - update 83. Geneva: WHO; March 2010. Available from http://www.who.int/csr/don/2010_01_15/en/index.html.
4. Cao B, Li XW, Mao Y, Wang J, Lu HZ, Chen YS et al. Clinical features of the initial cases of 2009 pandemic influenza A (H1N1) virus infection in China. N Engl J Med 2009; 24: 2507-17.
5. Perez-Padilla R, de la Rosa-Zamboni D, Ponce de Leon S, Hernandez M, Quiñones-Falconi F, Bautista E et al. Pneumonia and respiratory failure from swine-origin influenza A (H1N1) in Mexico. N Engl J Med 2009; 13: 680-9.
6. Turkish Ministry of Health. Pandemic coordination report. January 2010. Available from http://www.grip.gov.tr/images/stories/basin/05_ocakbulten.pdf (in Turkish).
7. Turkish Ministry of Health. Pandemic coordination report. January 2010. Available from: http://www.grip.saglik.gov.tr (accessed 18 January 2010).
8. Ajlan AM, Quiney B, Nicolaou S, Müller NL. Swine-origin influenza A (H1N1) viral infection: radiographic and CT findings. AJR Am J Roentgenol 2009; 193: 1494-9.
9. Agarwal PP, Cinti S, Kazerooni EA. Chest radiographic and CT findings in novel swine-origin influenza A (H1N1) virus (S-OIV) infection. AJR Am J Roentgenol 2009; 193: 1488-93.
10. Mollura DJ, Asnis DS, Crupi RS, Conetta R, Feigin DS, Bray M et al. Imaging findings in a fatal case of pandemic swine-origin influenza A (H1N1). AJR Am J Roentgenol 2009; 193: 1500-3.
11. Gill JR, Sheng ZM, Ely SF, Guinee DG, Beasley MB, Suh J et al. Pulmonary pathologic findings of fatal 2009 pandemic influenza A/H1N1 viral infections. Arch Pathol Lab Med 2010; 134: 235-43.
12. Ujita M, Renzoni EA, Veeraraghavan S, Wells AU, Hansell DM. Organizing pneumonia: perilobular pattern at thin-section CT. Radiology 2004; 232: 757-61.
13. Müller NL, Ooi GC, Khong PL, Zhou LG, Tsang KW, Nicolaou S. High-resolution CT findings of severe acute respiratory syndrome at presentation and after admission. AJR Am J Roentgenol 2004; 182: 39-44.